Contrasting photochemical and thermal reactivity of Ru(CO)2(PPh3)(dppe) towards hydrogen rationalised by parahydrogen NMR and DFT studies

Damir Blazina, John P Dunne, Stuart Aiken, Simon B Duckett, Charlotte Elkington, John E Mcgrady, Rinaldo Poli, Sue J Walton, M. Sabieh Sabieh Anwar, Jonathan A Jones, et al.

▶ **To cite this version:**

Damir Blazina, John P Dunne, Stuart Aiken, Simon B Duckett, Charlotte Elkington, et al.. Contrasting photochemical and thermal reactivity of Ru(CO)2(PPh3)(dppe) towards hydrogen rationalised by parahydrogen NMR and DFT studies. Dalton Transactions, 2006, 2006 (17), pp.2072-2080. 10.1039/B510616H . hal-03196074

HAL Id: hal-03196074
https://hal.science/hal-03196074

Submitted on 12 Apr 2021

HAL is a multi-disciplinary open access archive for the deposit and dissemination of scientific research documents, whether they are published or not. The documents may come from teaching and research institutions in France or abroad, or from public or private research centers.

L'archive ouverte pluridisciplinaire **HAL**, est destinée au dépôt et à la diffusion de documents scientifiques de niveau recherche, publiés ou non, émanant des établissements d'enseignement et de recherche français ou étrangers, des laboratoires publics ou privés.

Contrasting photochemical and thermal reactivity of $Ru(CO)_2(PPh_3)(dppe)$ towards hydrogen rationalised by parahydrogen NMR and DFT studies.

Damir Blazina, John P. Dunne, Stuart Aiken, Simon B. Duckett,* Charlotte Elkington, John E. McGrady,* Rinaldo Poli[c] Sue J. Walton, M. Sabieh Anwar[a], Jonathan A. Jones[a] and Hilary A. Carteret[b]

Department of Chemistry, University of York, Heslington, York YO10 5DD, UK. Phone: +441904432564; Fax: +441904435216; E-mail: sbd3@york.ac.uk

[a]*Centre for Quantum Computation, Clarendon Laboratory, University of Oxford, Parks Road, Oxford OX1 3PU, UK.*

[b]*Department of Combinatorics and Optimization, University of Waterloo, Waterloo, Ontario N2L 3G1, Canada*

[c] *Laboratoire de Chimie de Coordination (UPR CNRS 8241) 205 Route de Narbonne, 31077 Toulouse Cedex, France*

***This submission was created using the RSC Article Template* (*DO NOT DELETE THIS TEXT*)**
(*LINE INCLUDED FOR SPACING ONLY – DO NOT DELETE THIS TEXT*)

The synthesis, characterisation and thermal and photochemical reactivity of $Ru(CO)_2(PPh_3)(dppe)$ **1** towards hydrogen are described. Compound **1** proved to exist in both *fac* (major) and *mer* forms in solution. Thermally PPh_3 is lost from **1** in the major reaction pathway and the known complex $Ru(CO)_2(dppe)(H)_2$ **2** is formed. Photochemically, CO loss leading to products of the type $Ru(CO)(PPh_3)(dppe)(H)_2$ **3**, predominates over PPh_3 loss. The major isomer of **3**, viz. **3a**, contains hydride ligands that are *trans* to CO and *trans* to one of the phosphorus atoms of the dppe ligand. In a second isomer of **3** that is formed photochemically, both the hydride ligands are *trans* to distinct phosphines. **3a** failed to rearrange into the other form on the NMR timescale, although hydride site interchange is evident with activation parameters of $\Delta H^{\ddagger} = 95 \pm 6$ kJ mol^{-1} and $\Delta S^{\ddagger} = 26 \pm 17$ J K^{-1} mol^{-1}. DFT studies on model systems using PH_3 instead of PPh_3 and $H_2PCH_2CH_2PH_2$ instead of dppe were used to inform on the relative energies of the isomers of **1**, the products **3** and any potential 16 electron intermediates of the type $Ru(CO)_2(PH_3)(H_2PCH_2CH_2PH_2)$ or $Ru(CO)(PH_3)(H_2PCH_2CH_2PH_2)(PH_3)$ that might be involved in the formation of **3**.

Introduction

Transition metal complexes containing phosphine ligands have been widely employed as homogeneous catalysts[1] for transformations such as hydrogenation, hydroformylation, isomerisation and polymerisation, involving both alkene[2] and alkyne[3] substrates. Multidentate phosphines have attracted particular attention as auxiliary ligands because of their ability to control the molecular geometry of the resultant metal systems and hence enable both regio and stereo selectivity during catalytic transformations. In addition, the presence of multiple binding sites suppresses ligand dissociation and hence leads to longer catalyst lifetimes.[4]

A suitable example of this effect is provided by the photochemical reactions of complexes of the type $Ru(L)_4(H)_2$, where L is phosphine based. When $(L)_4 = P(CH_2CH_2PPh_2)_3$, the parent complex undergoes photochemical loss of dihydrogen and the resulting intermediate reacts rapidly with benzene to form the aryl hydride,[5] while on switching to $(L)_4 = (dppe)_2$ (dppe = $Ph_2CH_2CH_2Ph$) there is no evidence for C–H bond activation[6] despite the retention of the phenyl groups and the ethane backbone. In contrast, complexes containing primary phosphines, e.g. L = PMe_3, exhibit two distinct photochemical pathways involving loss of H_2 and phosphine, respectively.[7] Since the resulting $Ru(L)_4$ or $Ru(L)_3(H)_2$ intermediates can bind small molecules such as H_2, C_2H_4, CO and $HSiEt_3$, opportunities exist for such systems to achieve useful catalytic transformations.[8] For instance, Berry *et al.* have recently described how the related complex $Ru(PMe_3)_4(H)(SiMe_3)$ yields $Ru(PMe_3)_3(H)(SiMe_3)$, a 16 electron species that is capable of H-H, Si-H, C-H and Si-C bond activations.[9]

There have been several reports on the use of UV photolysis of a sample within the NMR probe to study *in-situ* reactions.[10,11] We have recently reported an investigation using this approach on the photochemical addition of hydrogen to complexes of the type $Ru(CO)_3(L)_2$, where L = PPh_3, PMe_3, PCy_3, P(*p*-tolyl)$_3$ and $AsPh_3$, together with studies on alkyne hydrogenation.[12] In this system, the reaction with hydrogen proceeds via the two competing processes shown in Scheme 1. The first of these involves the photochemical loss of CO, and preferential H_2 addition across the more π-accepting OC-Ru-CO axis of the resulting intermediate to form the *cis-cis-trans*-L isomer of $Ru(CO)_2(L)_2(H)_2$. In the second pathway, the single photon induces the loss of both CO and L, leading to the formation of an undetected 14 electron $Ru(CO)_2(L)$ fragment which reacts further to form detectable amounts of *cis-cis-cis* $Ru(CO)_2(L)_2(H)_2$ and $Ru(CO)_2(L)(solvent)(H)_2$, where solvent = toluene, THF and pyridine. In the case of L = PPh_3, *cis-cis-trans*-L $Ru(CO)_2(L)_2(H)_2$ proved to be an effective hydrogenation catalyst at elevated temperatures, with catalysis proceeding via initial loss of phosphine.[8,12]

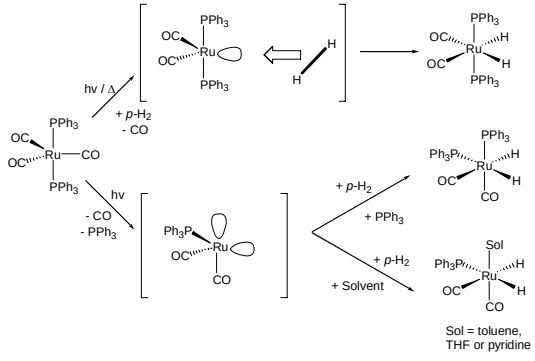

Scheme 1. Addition of hydrogen to $Ru(CO)_3(PPh_3)_2$.

We describe here studies on H_2 addition to the related Ru(0) system $Ru(CO)_2(PPh_3)$(dppe) which contains the chelating 1,2-bis(diphenylphosphino)ethane ligand. To study these transformations, we have employed NMR spectroscopy in conjunction with parahydrogen (p-H_2). The use of p-H_2 leads to the observation of PHIP (parahydrogen induced polarisation),[13] a well-established tool in mechanistic chemistry,[14] which allows low-concentration complexes, such as reaction intermediates, to be detected via enhanced ^{1}H NMR signals for nuclei that originate in the p-H_2 molecule. PHIP has yielded catalytic information for a number of mono-,[15] di-[16] and tri-nuclear[17] transition metal species. Recent achievements in this field include the sensitisation of a hydroformylation product containing a single p-H_2 atom,[18] transfer of polarisation via a ^{13}C nucleus to deuterium after the hydrogenation of a perdeuterated substrate,[19] and the investigation of *ortho-para* isomer interconversion and hydrogen isotope scrambling.[20] When in-situ laser flash photolysis of $Ru(CO)_3$(dppe) was used in conjunction with p-H_2, the hydride resonances seen for the product $Ru(CO)_2(dppe)_2(H)_2$ are enhanced by a factor of over 28,400 over their normal levels.[21] Such an approach has proved valuable in enabling p-H_2 to initialise a quantum computer[22] that is suitable for the implementation of quantum algorithms.[23] These reactions involve 18 electron, 5 coordinate precursors, which should be fluxional[24] and contain π acceptor ligands that are preferentially located in the equatorial plane.[25] The corresponding 16 electron intermediates that are generated from them by ligand loss are exemplified by $Ru(CO)_2(PMe^tBu_2)_2$, and $Ru(CO)_2(^tBu_2CH_2CH_2{}^tBu)$[26] which have trigonal bipyramidal structures with a vacant equatorial site.[27] However, these electron-deficient species are also fluxional, as a result of which, a number of H_2 addition products might be formed. In a previous paper, density functional theory was used to probe the potential energy surface for the corresponding reactions of H_2 with $Ru(CO)_3(H_2PCH_2CH_2PH_2)$ and $Fe(CO)_3(H_2PCH_2CH_2PH_2)$.[28] We now extend this analysis to the mixed carbonyl phosphine system, $Ru(CO)_2(PH_3)(H_2PCH_2CH_2PH_2)$, with the aim of understanding how the substitution of a carbonyl ligand by PH_3 perturbs the potential energy surface. In the case of the ruthenium complex, $Ru(CO)_3(H_2PCH_2CH_2PH_2)$, the triplet surface was shown to lie above the singlet at all points, so we restrict our attention to closed-shell states in the current system.

Experimental Section

General. All synthetic manipulations were carried out under an atmosphere of dry nitrogen using standard Schlenk, glove box or high vacuum techniques. Solvents were dried and distilled under nitrogen prior to use. $Ru(CO)_3(PPh_3)_2$ was prepared and purified using a literature procedure.[29] Other chemicals were purchased from commercial suppliers (Aldrich, Strem) and used without further purification.

Preparation of $Ru(CO)_2(PPh_3)$(dppe). The potential to prepare $Ru(CO)_2(PPh_3)$(dppe) from $Ru(CO)_3(PPh_3)_2$ has been described,[30] but the detailed synthetic procedure and full characterisation of the product were not communicated. In this study, $Ru(CO)_3(PPh_3)_2$ (100 mg, 0.14 mmol) and dppe (56 mg, 0.14 mmol) were refluxed in toluene (10 mL) under a continuous flow of N_2 for 45 min. The sample was then left to stand at room temperature for 12 hours, yielding a yellow microcrystalline precipitate of $Ru(CO)_2(PPh_3)$(dppe), which was then recrystallised from THF/pentane (1 : 2). Yield: 95 mg (82%). The characterisation data for this complex are given in Table 1. Analysis, C% 68.10 (found, 67.56 theoretical), H% 4.93 (found, 4.81 theoretical).

NMR methods. NMR solvents (Apollo Scientific) were dried using appropriate methods and degassed prior to use. The NMR measurements were made using NMR tubes fitted with J. Young Teflon valves and solvents were added by vacuum transfer on a high vacuum line. For the PHIP experiments, hydrogen enriched in the *para* spin state was prepared by cooling H_2 to 18 K over a paramagnetic catalyst (activated charcoal) using the system described previously.[21b] All NMR studies were carried out with sample concentrations of approximately 1 mM and spectra were recorded on a Bruker DMX-400 spectrometer with ^{1}H at 400.1, ^{31}P at 161.9 and ^{13}C at 100.0 MHz, respectively. ^{1}H NMR chemical shifts are reported in ppm relative to residual ^{1}H signals in the deuterated solvents (toluene-d_7, δ 2.13, and C_6D_6, δ 7.16), ^{13}C NMR relative to toluene-d_8, δ 21.3, CD_2Cl_2, δ 54.0 and C_6D_6, δ 128.4 and ^{31}P NMR in ppm downfield of an external 85% solution of phosphoric acid. Modified COSY, HMQC and EXSY pulse sequences were used as previously described.[16,31] ^{1}H EXSY spectra used to obtain kinetic data were processed using literature methods[32] and analysed for simple two-site exchange processes.[33]

In-situ photolysis. This was achieved using a modified NMR probe that was equipped for *in–situ* photolysis, as described previously.[11] A Kimmon IK3202R-D 325 nm He–Cd 27 mW continuous wave (CW) laser was used as the light source.

Computational details. All calculations were performed using the Gaussian 03[34] program together with the modified form of the B3PW91 functional in conjunction with a flexible polarisable basis sets.[35] Specifically, the c_3 coefficient in Becke's original three–parameter fit to thermochemical data[36] was changed to 0.15, to give the B3PW91* functional. Atoms C, O and P were described by the triple–zeta basis sets of Schäfer et al.[37] augmented by one d polarisation function (α = 0.8, 1.2 and 0.55 respectively). The Ru atom was described with the SDD basis set,[35] which uses the Stuttgart/Dresden ECP and double–zeta functions for all valence electrons, augmented with an f polarisation function (α = 1). All minima were fully optimised and characterised by computing vibrational frequencies at the same level of theory. The calculations reported here used the same level of theory previously employed for $Fe(CO)_2(PH_3)_2$,[38] where a benchmark investigation demonstrated that it gave the most reliable results for $Fe(CO)_4$.[39] In all cases, the phenyl groups on PPh_3 and dppe are replaced by hydrogens.

Results and discussion

The $Ru(CO)_2(PPh_3)$(dppe) **1** used here was prepared and purified as described in the Experimental section, and IR (ν_{CO}), NMR and FAB mass spectral data are collected in Table 1. Assuming that the dppe ligand spans one axial and one equatorial site, there are two possible isomers of 1, one with an axial phosphine (**1a**) and one with an axial carbonyl (**1b**) (Figure 1). At 295 K, two distinct signals were observed in the ^{31}P NMR spectrum at δ 57 (PPh_3) and 70.3 (dppe), the equivalence of the two dppe phosphorus centres clearly indicating that the molecule is fluxional. Moreover, the presence of three ν(CO) bands in the spectrum of **1** confirms that more than one species is present in solution. As the temperature was lowered, the δ 70.3 signal broadened and collapsed into the baseline before appearing again as two broad signals at δ 79.6, 60.6. Even at 183 K, these signals remained broad which precluded the determination of exact J_{PP} couplings. However, a large (200 Hz) *trans* coupling connected the signal at δ 79.6 and the resonance at 57.8 (PPh_3), confirming that **1a**, where there is a *trans* arrangement between the PPh_3 ligand and one of the ^{31}P centres on the dppe ligand, is the dominant form at low temperature. In addition, two further, less intense and very broad resonances were observed at ca. δ 32.1 and 27.5. These could not be resolved fully due to the limitations imposed by the freezing point of the NMR solvent, toluene-d_8, but clearly indicate the presence of a second isomer, presumably **1b**.

A survey of the potential energy surface for the model complex $Ru(CO)_2(PH_3)(H_2PCH_2CH_2PH_2)$ (**1'**) confirms the presence of two distinct local minima, **1a'** and **1b'** (Figure 1), lying within 1.5 kJ mol^{-1} of each other. Previous computational studies on the closely related species $Ru(CO)_2(PH_3)_3$ haved located almost

isoenergetic structures analogous to **1a'** and **1b'**, along with a third isomer where both CO ligands are in the axial positions, some 12.7 kJ mol^{-1} higher in energy.[40,41,41] We have been unable to locate a third minimum in the current system, presumably because the dppe ligand is unable to bridge the 120º angle between the two equatorial sites. The (unscaled) C-O vibrational frequencies of **1a**' and **1b'** (1977, 2015 cm^{-1} and 2001, 2055 cm^{-1}, respectively) also offer an explanation for the presence of three, rather than four, ν(C-O) bands in IR spectrum: the 2015 cm^{-1} band (symmetric stretch) of **1a'** is very weak and is likely to be obscured by the more intense 2001 cm^{-1} of **1b'** (antisymmetric stretch).

Table 1. Spectroscopic data for $Ru(CO)_2(PPh_3)$(dppe) **1**. IR spectra were recorded in hexane, ^{13}C NMR spectra in CD_2Cl_2 and all other NMR spectra in C_6D_6 at 295 K.

IR (ν_{CO}) / cm^{-1}	2049 (m), 2027 (m), 1897 (m)
Molecular ion / m/z	789
^1H NMR	2.16, d, J_{PH} = 19 Hz
	6.90-7.20 (m)
	7.60 (m)
^{31}P {^1H} NMR	57.0 (1P), t, J_{PP} = 83 Hz
	70.3 (2P), d, J_{PP} = 83 Hz
^{13}C {^1H} NMR	32.2, m (CH_2)
	129, m
	134, m
	138.7, d, J_{CP} = 24 Hz
	138.5, d, J_{CP} = 26 Hz
	216, br (CO)

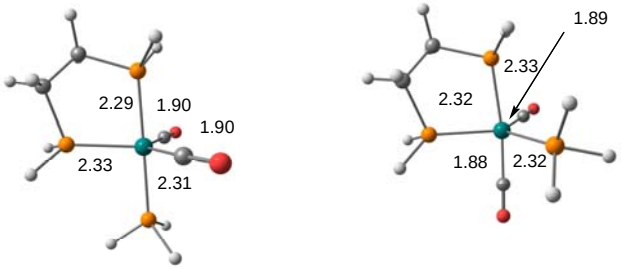

1a' E_{rel} = +1.5 kJ mol^{-1} **1b'** E_{rel} = 0 kJ mol^{-1}

Figure 1. Optimised structures and relative energies for the two stable isomers of $Ru(CO)_2(PH_3)(H_2PCH_2CH_2PH_2)$. Bond lengths are in Å.

Thermal reactions of $Ru(CO)_2(PPh_3)$(dppe) 1 with *p*-H_2: When compound **1** was warmed to 315 K with *p*-H_2 in C_6D_6, two enhanced NMR signals were observed in the hydride region of the ^1H NMR spectrum at δ –7.55 and –6.32. These signals have the same chemical shifts and profiles as the known compound $Ru(CO)_2$(dppe)$(H)_2$, **2**.[42] When this experiment was repeated in the presence of 2 atm. of CO, the relative intensities of these hydride resonances were unaffected, but the signals were quenched by the addition of a 10-fold excess of PPh_3. It can therefore be concluded that **1** reacts thermally with H_2 via initial PPh_3 loss. The thermal loss of a phosphine from $Ru(CO)_2(PEt_3)_3$ and related systems has been successfully used in the past to prepare the analogous dihydrides, $Ru(CO)_2(PEt_3)_2(H)_2$.[41]

Photochemical reactions of $Ru(CO)_2(PPh_3)$(dppe) 1 with H_2: An NMR sample of **1** in C_6D_6 under 3 atm. *p*-H_2 was prepared and exposed to broad band UV irradiation from a medium pressure Hg-Arc lamp for 5 minutes outside the NMR spectrometer. When this sample was examined by ^1H NMR spectroscopy the characteristic resonances of **2** were again observed, along with those of a second dihydride, **3a**, the ratio between the two species being 0.78 : 1. The hydride resonances of **3a** at δ –7.00 and –7.56 correspond to those of the [OC-6-42][43] isomer of Ru(CO)(dppe)$(PPh_3)(H)_2$ (Figure 2, Table 2) , the synthesis and characterisation of which has been reported previously by Garrou *et al.* and Onishi *et al.*[44] A more detailed characterisation of the resonances of **3a** using PHIP is reported in the next section, but the most significant point to note at this stage is that the presence of **3a** in solution suggests that photochemically induced CO loss from **1** leads to the formation of a stable dihydride complex. After 60 minutes further UV irradiation, the complete loss of the ^{31}P signal due to **1** indicated its complete conversion into **2** and **3a**. When this sample was warmed in the NMR spectrometer from 295 K to 373 K, the hydride signals for **2** in the corresponding ^1H NMR spectra were enhanced, while those for **3a** were unaffected. The absence of *p*-H_2 enhancement suggests that the hydride ligands of **2**, but not **3a**, exchange with H_2 under thermal conditions.

***In-situ*-photochemical reactions of $Ru(CO)_2(PPh_3)$(dppe) 1 with *p*-H_2: detection and characterisation of isomeric products.** In order to explore the photochemical reaction pathway in more detail, we used an *in-situ* approach in conjunction with *p*-H_2. When a sample of **1** was exposed to *p*-H_2 with concurrent UV laser photolysis at temperatures of 263 K and above, hydride signals for **2** and **3a** were again visible, along with two new products, **3b** and **4** (Figure 2, Table 2). However, once the sample was allowed to come to thermal equilibrium only the signals due to **2** and **3a** remained, indicating that **3b** and **4** are formed under kinetic control. The four additional hydride resonances from **3b** and **4** were characterised by multidimensional NMR spectroscopy (a typical *p*-H_2 enhanced spectrum is shown in Figure 3).

Table 2. NMR data for three isomers of Ru(CO)(dppe)$(PPh_3)(H)_2$ produced upon the irradiation of $Ru(CO)_2(PPh_3)$(dppe) **1** with H_2 in C_6D_6 at 295 K. The labelling of the atoms is shown in Figure 2.

	δ (^1H)	δ (^{31}P{^1H})
3a	–7.00 (H_a), dddd, J_{HP} = 78 Hz (P_b), 22 Hz (P_a), 19 Hz (P_c), J_{HH} = –5 Hz	61.4 (P_a), dd, J_{pp} = 240 Hz (P_c), 18 Hz (P_b)
	–7.56 (H_b), dddd, J_{HP} = 27 Hz (P_b), 25 Hz (P_a), 20 Hz (P_c), J_{HH} = –5 Hz	66.9 (P_b), dd, J_{PP} = 18 Hz (P_a), 3 Hz (P_c)
		81.7 (P_c), dd, J_{PP} = 240 Hz (P_a), 3 Hz (P_b)
3b	–6.54 (H_a), m (*trans* to P_b),[a] J_{HH} = –5 Hz	47.3 (P_a)
		64.5 (P_b)
	–9.22 (H_b), dddd, J_{HP} = 65 Hz (P_a), 35 Hz (P_c), 17 Hz (P_b), J_{HH} = –5 Hz	83.2 (P_c)
4	–7.17 (H_a), dddd, J_{HP} = 79 Hz (P_b), 24 Hz (P_a), 18 Hz (P_c), J_{HH} = –4.5 Hz	77.5 (P_a), dd, J_{pp} = 14, 230 Hz
		66.7 (P_b), d, J_{pp} = 14 Hz
		55.4 (P_c), dd, J_{PP} = 66, 230 Hz
	–8.42 (H_b), dq, J_{HP} = 27 Hz, J_{HH} = –4.5 Hz	30.7 (P_d), d, J_{PP} = 66 Hz

The basic features of the ^{31}P NMR spectrum of **3a** have been described above, but the *p*-H_2 enhancement reveals much greater detail, and a number of unusual features. While the hydride resonances of **3a** show anitiphase character due to PHIP, the splittings (Figure 3) are consistent with couplings to three phosphorus centres. However, when a ^1H-^{31}P HMQC experiment was recorded to locate the corresponding ^{31}P chemical shifts, a total of six cross-peaks were detected at δ 46.4, 61.4, 66.9, 76.1, 81.7 and 87.2 (see Figure 4). We note that Heaton *et al*. have observed additional resonances in HMQC spectra of rhodium carbonyl clusters, and attributed them to double and triple quantum coherence effects.[45] Single quantum transitions (revealing real ^{31}P chemical shifts) can be selectively enhanced using a magnetisation transfer delay to $1/(5\times J_{HX})$, rather than the conventional $1/(2\times J_{HX})$. Three cross-peaks remain visible in this experiment, to signals at δ 61.4, 66.9 and 81.7 (Figure 4), which can be shown to be real by direct decoupling. In contrast, setting

the delay to $1/(J_{HX})$ leads to the observation of only the triple quantum coherence "artefacts" at δ 46.4, 76.1 and 87.2 for **3a** (Figure 4).

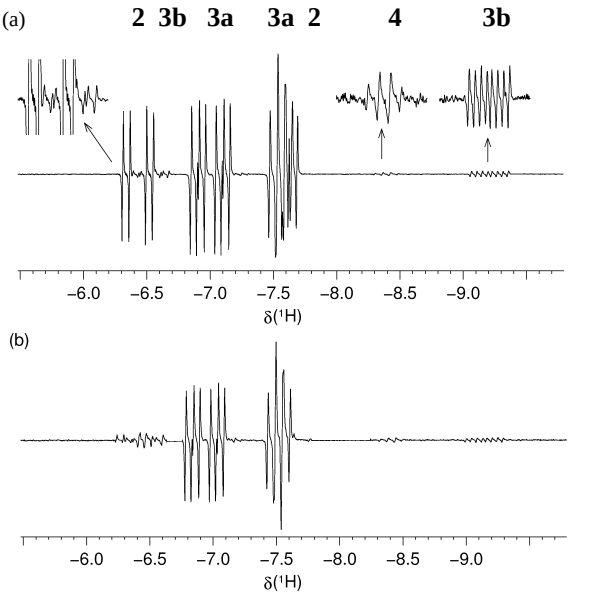

Figure 3. Hydride region of the ^{1}H NMR spectrum of 1 in C_6D_6 under 3 atm of *p*-H_2: (a) at the onset of photolysis; (b) after 20 min of photolysis. The resonances marked * are due to $Ru(CO)_2(dppe)(H)_2$.

The hydride resonance of **3a** that appears at δ –7.00 exhibits a large *trans* $^2J_{HP}$ coupling of 78 Hz (to a ^{31}P nucleus resonating at δ 66.9) and two *cis* $^2J_{HP}$ couplings of 19 and 22 Hz (to ^{31}P nuclei resonating at δ 87.1 and 61.4, respectively). The second hydride resonance of **3a** at δ –7.56, exhibits three *cis* $^2J_{HP}$ couplings of 27, 20 and 25 Hz to the same three ^{31}P nuclei, respectively (see Table 2 for a summary of NMR data). In addition, the ^{31}P signals at δ 61.4 and 81.7 exhibit a large 240 Hz coupling in a high-resolution ^{1}H-^{31}P HMQC experiment, indicating that the associated nuclei are distinct and mutually *trans*. One of these nuclei is therefore due to the PPh_3 ligand, while the other originates from one of the arms of the dppe moiety. The hydride site which yields the δ –7.56 signal is therefore *trans* to a CO ligand. The phosphorus nucleus resonating at δ 61.4 also interacts with the third ^{31}P centre resonating at δ 66.9 in the form of an 18 Hz coupling, a value that indicates these two nuclei are mutually *cis*. The signals at δ 66.9 and 81.7 both showed a very small additional coupling of 3 Hz. These resonances come from the dppe ligand, and the small coupling is the result of cancellation of the $^2J_{PP}$ coupling through the metal centre and the $^3J_{PP}$ coupling through the ethane backbone of the dppe ligand; these two couplings are of opposite sign. Such situations have been reported previously.[42,46]

The new species **3b** exhibits enhanced hydride signals at δ –6.54 and –9.22 and has not been observed previously. The hydride signal at δ –9.22 appears as a doublet of doublets of doublets of antiphase doublets with a large *trans* $^2J_{HP}$ of 65 Hz arising from a ^{31}P nucleus that resonates at δ 47.3. The two additional *cis* couplings of 35 and 17 Hz arise from the ^{31}P centres that were detected at δ 83.2 and 64.5, respectively, in the HMQC experiment. The multiplicity of the lower field hydride could not be determined directly because of signal overlap with **2**, although a $^2J_{HH}$ of –5 Hz could be resolved, and a *trans* ^{31}P nucleus found at δ 64.5. These NMR data are, however, sufficient to identify this compound as **3b**, an isomer of **3** where one hydride is *trans* to the PPh_3 ligand and the other is *trans* to one of the ^{31}P centres of the dppe moiety. From chemical shift trends in **3a** and **3b** (vide infra), the ^{31}P signal at δ 47.3 is

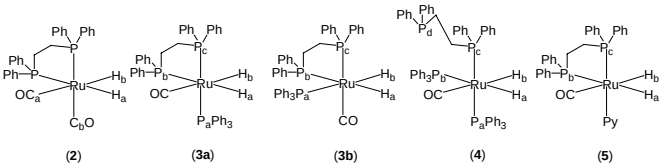

Figure 2. Proposed structures and atom labelling for the complexes detected in this study using parahydrogen methods.

assigned to the PPh_3 ligand while the other two correspond to dppe signals. We note that a species analogous to **3b** has been detected upon irradiation of the related complex $Ru(CO)_3(PhP(CH_2CH_2PPh_2)_2)$ with H_2.[47]

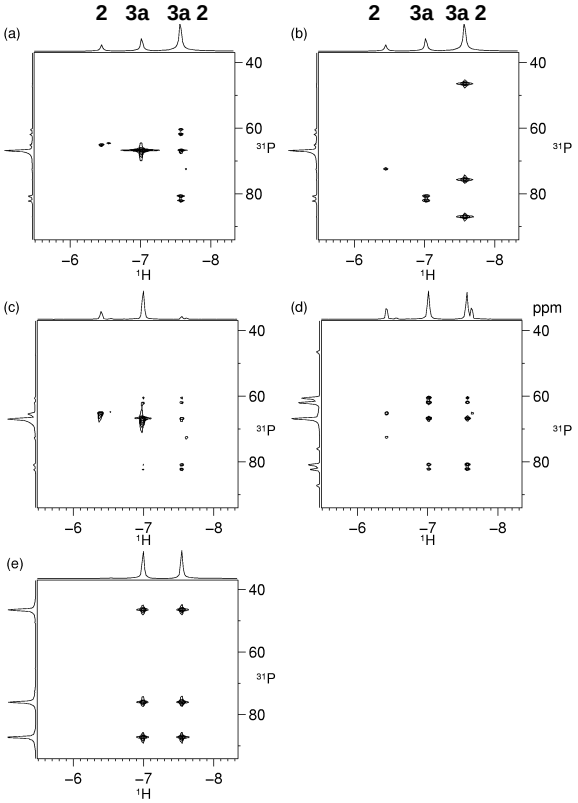

Figure 4. ^{1}H-^{31}P HMQC experiments for products obtained from **1** in C_6D_6 with concurrent laser photolysis under 3 atm of *p*-H_2: (a) with a conventional delay ($1/2\times J_{HP}$), optimised for *trans* couplings; (b) with a conventional delay ($1/2\times J_{HP}$), optimised for *cis* couplings; (c) optimised for *trans* couplings with a delay of $1/(5\times J_{HP})$; (d) optimised for *cis* couplings with a delay of $1/(5\times J_{HP})$; (e) with a delay of $1/J_{HP}$. Traces "c" and "d" show the real ^{31}P chemical shifts, while trace "e" shows the cross-peaks due to triple quantum coherence effects.

The ratio of hydride resonance intensities seen for **3a** : **2** varies with irradiation time, progressively increasing from the initial value of 2.2 : 1 to 20 : 1 after 20 min irradiation (see Figure 3). In contrast, the observed ratio of the hydride signal intensities for **3a**, **3b** and **4** remains essentially constant over the course of the experiment at 1 : 0.04 : 0.02. There are two possible explanations for this observation; (1) **2** reacts photochemically with free PPh_3 to form **3a**, **3b** and **4** , leading to increased concentrations of the latter or (2) photolysis of **3a** at 325 nm leads to exchange of hydrides with free H_2, while **2** is inert. In this case, the enhanced intensity of the signal for **3a** does not reflects a greater concentration of this species, but rather the fact that the polarisation is continually regenerated by the binding of fresh p-H_2. When an authentic sample of **2** was prepared and photolysed at 325 nm in the presence of *p*-H_2 and PPh_3, no evidence for the formation of **3** was observed; indeed, there was no *p*-H_2 activity. In contrast, when a sample of **3a** was prepared and photolysed at 325 nm in the presence of *p*-H_2, the corresponding hydride resonances of **3a** and **3b** appeared as PHIP enhanced signals in the ratio 1 : 0.04. Since the hydride

resonances of **3a** failed to show PHIP prior to photolysis, and **3b** was not visible, it can be concluded that secondary photolysis of **3a** affects the distribution of products.

The final product observed in this reaction, **4**, was characterised by two *p*-H_2 enhanced hydride signals at δ -7.17 and –8.42 that arise from two chemically distinct hydride ligands (Figure 3 clearly shows the high field signal, the second resonance is masked in this spectrum). This new species was detectable at the end of the experiment in very low concentrations (ca 5% of the level of **3a**). The multiplicities of the hydride signals for **4** are identical to those of **3a**, which suggests that it is also a *tris*-phosphine complex, but, at very long collection times, a total of *four* distinct ^{31}P resonances were observed in the corresponding $^{31}P\{^1H\}$ NMR experiment,. The presence of one of these resonances in a region corresponding to a non-coordinated phosphorus centre (δ 30.7) confirms that one arm of the dppe ligand has decoordinated (Table 4), leaving the second phosphorus centre of the dppe in an axial site *trans* to a PPh_3 ligand. Given that the formation of **2** involves the liberation of PPh_3 it is not surprising that **4** can be formed.

In summary, it is clear from these data that the novel *in-situ* photochemical approach employing parahydrogen allows us to observe a reaction product whose concentration is too low to allow its detection by conventional NMR spectroscopy. The exact mechanism of formation of **2**, **3a**, **3b** and **4**, however, remains to be established.

The ^1H NMR signals for the hydride ligands of **3a** proved to be of an intensity which indicated that 67.1%† of the *p*-H_2 spin state was conserved during the addition process. This compares with the value of 89.8 % for $Ru(CO)_2(dppe)_2(H)_2$.[21]

Evidence for a 14-electron intermediate: effect of added pyridine on the irradiation of 1 with *p*-H_2: In previous studies of the photochemistry of $Ru(CO)_3(L)_2$, it has been shown that a second single-photon process induces loss of both CO and L from $Ru(CO)_3(L)_2$. This process competes with CO dissociation from $Ru(CO)_3(L)_2$ and leads to the formation of *cis–cis–cis* $Ru(CO)_2(L)_2(H)_2$ via reaction of the solvent complex $Ru(CO)_2(L)(solvent)(H)_2$ (where solvent = toluene, THF and pyridine) with CO. In order to explore whether a similar double ligand loss process was also operative in this case, we investigated the *in-situ* irradiation of **1** in C_6D_6 solutions containing both *p*-H_2 and pyridine. Under these conditions, at the onset of photolysis, the two isomers of **3** are observed in the same ratio seen for the corresponding reaction without pyridine. The proportion of **3a** relative to **2** also remained the same at 2.2 : 1 (based on the *p*-H_2 enhanced hydride signals) regardless of the concentration of pyridine. In the pyridine doped spectra two hydride resonances of the previously reported double substitution product OC-6-13 (Figure 2) isomer of $Ru(H)_2(CO)(dppe)(pyridine)$, **5**, were also detected at δ –4.17 and –4.57.[12] The ratio of the hydride resonance signal intensities for **3a** : **5** were 1 : 0.11 for an 18 fold excess and 1 : 0.2 for a 61 fold excess of pyridine. The higher concentrations of pyridine therefore substantially increase the proportion of $Ru(H)_2(CO)(dppe)(pyridine)$ formed in this reaction and suggest that a process whereby both CO and PPh_3 are lost from **1** competes with the loss of PPh_3 and CO. When a sample of **3a** was irradiated in C_6D_6 containing a 60 fold excess of pyridine and *p*-H_2, the hydride resonances for **5** again appeared. The ratio of **3a** : **5** (1 : 0.01), was, however, dramatically lower than the ratio when **1** is the precursor, suggesting that photolysis of **3a** is not the major source of **5**. On this basis, we conclude that a minor photochemical pathway involving the dissociation of both CO and PPh_3, followed by the net recoordination of either CO or PPh_3 and the activation of H_2 contributes to the observed product distribution. Given the constant ratio of **3a** : **3b**, even in the presence of pyridine, it seems likely that both the single and two ligand loss pathways ultimately proceed via a common intermediate.

DFT analysis of the potential energy surface of $Ru(H_2PCH_2CH_2PH_2)(PH_3)(CO)(H)_2$

Density functional theory has been used to explore the potential energy surfaces of both **2** and **3**, using model systems (denoted **2'** and **3'**) where the phenyl groups have been replaced by hydrogens. For dicarbonyl dihydride species, **2'**, three distinct minima have been located, the most stable being those with *cis* dihydrides, **2a'** and **2b'**. Of these, the former is 9 kJ mol^{-1} lower in energy, consistent with the structure of **2** proposed above. A total of four distinct isomers have been located for **3'**. The two most stable, **3a'** and **3b'** correspond to the experimentally observed species, and lie within 1 kJ mol^{-1} of each other, consistent with their coexistence in solution. Both are formally related to **2a'** through substitution of one of the two chemically distinct CO groups by PH_3. The remaining two isomers, **3c'** and

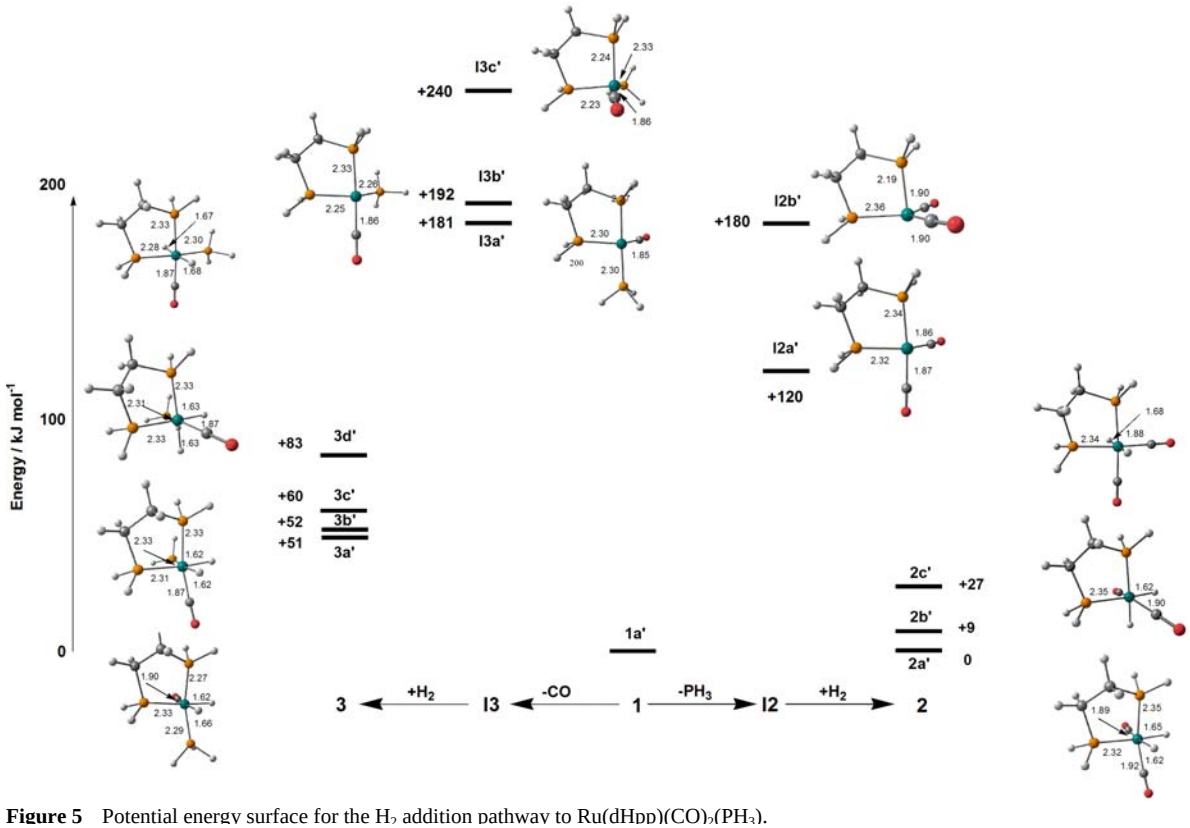

Figure 5 Potential energy surface for the H_2 addition pathway to $Ru(dHpp)(CO)_2(PH_3)$.

3d', lie 9 kJ mol^{-1} and 32 kJ mol^{-1}, above **3a'**, and have not been observed in any of our experiments.

Mechanism of formation of 2, 3 and 4: The mechanism of addition of H_2 to the closely related complexes $Ru(CO)_3(L)_2$ (where L is a monodentate phosphine) has been studied previously,[12] and shown to involve CO loss followed by H_2 addition to the resultant 16 electron intermediate. The preferred direction of attack appears to be across the more strongly accepting OC-Ru-CO axis, yielding the *cis–cis–trans*-L isomer of $Ru(CO)_2(L)_2(H)_2$. The electronic structure of $Ru(dppe)(CO)_2$ has been discussed in a previous paper,[28] and numerous closely related 16-electron species such as RuL_4[15,27,44–46,49,48] and $Ru(CO)_2(L)_2$ [27,46] have also been studied using theoretical techniques. Optimised structures and relative energies of the two model intermediates, **I2'** and **I3'**, arising from loss of PH_3 and CO from **1'**, respectively, are summarised in Figure 5. In all cases, the energies are given relative to the most stable isomer of **1'** (**1b'**).

For the intermediate arising from PH_3 loss, two distinct isomers, **I2a'** and **I2b'**, have been located, with vacancies in the equatorial and axial sites of the parent trigonal bipyramid, respectively. The former is more stable by 61.6 kJ mol^{-1}, indicating that it will be the only isomer present under the experimental conditions. In contrast, loss of a CO ligand from **1** leads to two distinct isomers, **I3a'** and **I3b'**, both of which have a vacancy in the equatorial plane, the former with an axial phosphine, the latter with an axial CO ligand. **I3a'** lies 11.1 kJ mol^{-1} lower than **I3b'**, consistent with the general preference for the stronger π-acceptor ligands to occupy equatorial sites, and suggesting that, under experimental conditions, **I3a** will be the dominant intermediate arising from CO loss. Sargent and Hall have investigated the oxidative addition of H_2 to square-planar $IrCl(CO)(PH_3)_2$,[49] and showed that addition across the P-Ir-P, rather than Cl-Ir-CO, axis leads to a more stable transition state, although the inclusion of methyl groups on the phosphine ligand reversed this trend. We have been unable to locate any transition states for H_2 addition in this case, suggesting that the reaction is barrierless. We therefore propose that **3a** and **3b** are formed *via* approach of H_2 aligned along the axial and equatorial planes of **I3a**, respectively (Scheme 2). Significantly, the opening of the equatorial C-Ru-P angle to 155^o in **I3a** means that the axial and equatorial axes are not strongly differentiated.

Finally, we note that the calculated total energies for the reactions **1' → I2'** + PH_3 and **1' → I3'** + CO (taking the lowest energy isomer in each case) are 120 kJ mol^{-1} and 183 kJ mol^{-1}, respectively, clearly indicating that loss of PH_3 to form the dicarbonyl species is the thermodynamically favoured outcome. The computed energies are therefore consistent with the exclusive formation of $Ru(dppe)(CO)_2(H)_2$ **(2)**, and not $Ru(dppe)(CO)(PPh_3)(H)_2$ (**3**), under thermal conditions.

Hydride site interchange in $Ru(dppe)(PPh_3)(CO)(H_2)$ (3): Many dihydride complexes have been found to undergo intramolecular exchange of hydride ligand sites. proposed rearrangement pathways include tunneling,[50,51,52] trigonal twist,[53] the formation of formyl intermediates,[54,55,56] and the reversible formation of a transition state featuring significant shortening of the H-H distance or a thermally accessible η^2-H_2 intermediate with trigonal bipyramidal shape.[57] Our previous analysis of the potential energy surface for **2** is consistent with the last of these, revealing two distinct transition states leading to hydride exchange, both of which are best described as dihydrogen complexes of zerovalent $Ru(CO)_2(PH_2CH_2CH_2PH_2)$.[28,42] The two pathways, corresponding to clockwise and anticlockwise rotations of the H_2 unit, have computed activation parameters of $\Delta H^{\ddagger}$ = 82 kJ mol^{-1}, $\Delta S^{\ddagger}$ = -0.2 J mol^{-1} K^{-1} and $\Delta H^{\ddagger}$ = 78.6 kJ mol^{-1}, $\Delta S^{\ddagger}$ = -0.6 J mol^{-1} K^{-1}, in good agreement with the experimentally determined $\Delta H^{\ddagger}$ value of 85.5 ± 2 kJ mol^{-1}. A similar analysis of the potential energy surface for **3a** also reveals two distinct transition states, **TSa** and **TSb**, corresponding to clockwise and anticlockwise rotations of the H_2 unit about a $Ru(CO)(PH_3)(PH_2CH_2CH_2PH_2)$ fragment (Figure 6).

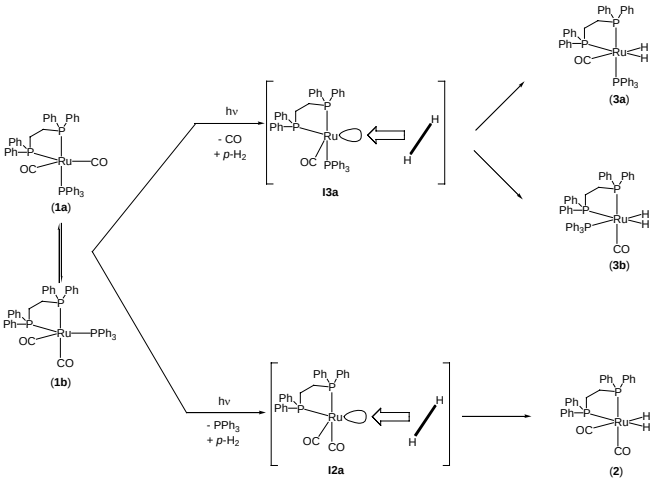

Scheme 2. Possible mechanisms for photochemical formation of **2**, **3a** and **3b** from $Ru(CO)_2(PPh_3)(dppe)$ **1** and *p*-H_2.

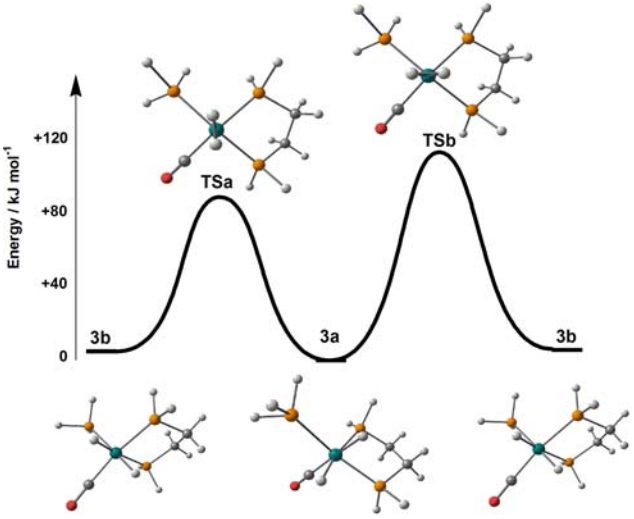

Figure 6. Potential energy surface for hydride exchange in **3a**.

Both processes, however, lead to interconversion of **3a** and **3b**, and a 180° rotation, passing through both transition states *and* **3b**, is required to exchange the hydrides in **3a**.

We used EXSY spectroscopy to probe the dynamic behaviour of the hydride ligands of **3a**. At 343 K, the on-set of a process wherein the two-hydride ligands interchanged sites was observed (k = 0.68 s^{-1}). A series of 1D-EXSY NMR experiment where the temperature was varied between 346 and 373 K yielded activation parameters of $\Delta H^{\ddagger}$ = 95 ± 6 kJ mol^{-1} and $\Delta S^{\ddagger}$ = 26 ± 17 J K^{-1} mol^{-1} ($\Delta G^{\ddagger}_{350}$ = 86.2 ± 0.1 kJ mol^{-1}). In order to learn more about the nature of the exchange process, fully coupled ^{1}H-2D-NOESY and ^{31}P-2D-NOESY NMR spectra were recorded. Although hydride exchange was clearly evident in the ^{1}H spectrum, no exchange peaks were observed in the ^{31}P spectrum. The EXSY methods revealed no evidence for H_2 elimination in

3a, even at 378 K, consistent with that fact that the hydride resonances for **3a** failed to show PHIP at this temperature. Even in a high signal to noise EXSY run, no evidence for the interchange of **3a** into **3b** was observed. We therefore conclude that the concentration of the **3b** intermediate must be undetectably low, consistent with the fact that it has only ever been observed under *p*-H_2 enhancement. The highest point on the potential energy surface, **TSb**, lies 112 kJ mol^{-1} above **3a**, a rather higher barrier than the 95 kJ mol^{-1} obtained from the experiment, probably due to the neglect of the bulky phosphine substituents, but the trend towards slower exchange in **3** than **2** is clearly reproduced.

Finally, we note that Mann and co-workers have previously reported the exchange of hydride ligands in $Ru(CO)(H)_2(PPh_3)_3$ on the NMR timescale,[53] and suggested that this process occurred via a trigonal twist mechanism. We have located a trigonal twist transition states that exchanges the two hydrides in **3a** without formation of **3b**, only 11 kJ mol^{-1} above **TSa**. This process would, however, also lead to exchange of the dppe phosphines, clearly contrary to experiment. We therefore conclude that the presence of the chelating phosphine perturbs the potential energy surface in such a way that the trigonal twist is disfavoured relative to the pathway illustrated in Figure 6.

Conclusions

In this paper we have described the synthesis of $Ru(CO)_2(PPh_3)$(dppe) **1**, which proved to exist in both *fac* and *mer* forms in solution. Under thermal conditions, **1** selectively loses PPh_3 and reacts with H_2 to yield $Ru(CO)_2$(dppe)$(H)_2$ **2**. However, upon 325 nm photolysis, CO loss dominates PPh_3 loss by a factor of 2.2, giving rise to two distinct isomers of $Ru(CO)(PPh_3)$(dppe)$(H)_2$ **3** and the PPh_3 addition product $Ru(CO)(PPh_3)_2(\eta^1$-dppe$)(H)_2$ **4.** Irradiation of **1** with H_2 in the presence of pyridine reveals the presence of a minor photochemical process involving CO and PPh_3 loss which leads to $Ru(H)_2(CO)$(dppe)(pyridine) **5**. The major isomer of **3** contains hydride ligands *trans* to CO and one of the phosphines of the dppe ligand. In the second isomer, both hydrides lie *trans* to phosphine. The potential energy surface optimised using density functional theory is fully consistent with the observed products, and provides insight into the mechanisms by which they are formed.

Acknowledgements

We are grateful to the EPSRC and the European Union (HYDROCHEM network, contract HPRN-CT-2002-00176) for funding, as well as to Prof. R. N. Perutz, Dr. R. J. Mawby and Dr. J. M. Lynam for helpful discussions. Experimental assistance from Ms. K. A. M. Ampt, Ms. N. J. Smith and Mr. N. J. Wood is gratefully acknowledged.

References

† Electronic supplementary information (ESI) available: xxx See http://www.rsc.org/suppdata/dt/

1. C. Bianchini, A. Meli, M. Peruzzini, F. Vizza, P. Frediani, J. A. Ramirez, *Organometallics* **1990**, *9*, 226.
2. (a) D. L. Dubois, D. W. Meek, *Inorg. Chim. Acta* **1976**, *19*, L29. (b) C. Bianchini, C. Mealli, A. Meli, M. Peruzzini, F. Zanobini, *J. Am. Chem. Soc.* **1988**, *110*, 8725. (c) C. Bianchini, A. Meli, M. Peruzzini, F. Vizza, Y. Fujiwara, T. Jintoku, H. Taniguchi, *J Chem. Soc. Chem. Commun.* **1988**, 210. (d) C. Bianchini, F. Laschi, A. Meli, M. Peruzzini, P. Zanello, P. Frediani, *Organometallics* **1988**, *7*, 2575.
3. (a) C. Bianchini, P. Frediani, A. Meli, F. Vizza, M. Peruzzini, F. Zanobini, *Organometallics* **1989**, *8*, 2080. (b) T. E. Muller, M. Grosche, E. Herdtweck, A.-K. Pleier, E. Walter, Y.-K. Yan, *Organometallics* **2000**, *19*, 170.
4. (a) J. A. Osborn, J. F. Young, G. Wilkinson, *J. Chem. Soc. Chem. Commun.* **1965**, 17. (b) H. A. Mayer, W. C. Kaska, *Chem. Rev.* **1994**, *94*, 1239.
5. R. Osman, D. I. Pattison, R. N. Perutz, C. Bianchini, J. A. Casares, M. Peruzzini, *J. Am. Chem. Soc* **1997**. *119*, 8459.
6. L. Cronin, M. C. Nicasio, R. N. Perutz, R. G. Peters, D. M. Roddick, M. K. Whittlesey, *J. Am. Chem. Soc.* **1995**, *117*, 10047.
7. V. Montiel-Palma, R. N. Perutz, M. W. George, O. S. Jina, S. Sabo-Etienne, *Chem. Commun.* **2000**, 1175.
8. (a) D. Evans, J. A. Osborn, F. H. Jardine, G. Wilkinson, *Nature* **1965**, *208*, 1203. (b) D. Evans, J. A. Osborn, G. Wilkinson, J. Chem. Soc. A **1968**, 3133. (c) R. A. Sanchez-Delgado, J. S. Bradley, G. Wilkinson, *J. Chem. Soc. Dalton Trans.* **1976**, 399.
9. V. K. Diourmaev, L. J. Procopio, P. J. Carroll, D. H. Berry. *J. Am. Chem. Soc.* **2003**, *125*, 8043
10. (a) S. Geftakis, G. E. Ball, *J. Am. Chem. Soc.* **1999**, *121*, 6336. (b) N. A. Knatochnil, J. A. Pachinson, P. J. Bedmaishi, P. J. Sadler, *Angew. Chem. Int. Ed.* **1999**, *38*, 1460. (c) C. E. Lyon, J. L. Lopez, B. M. Cho, P. J. Hore, *Mol. Phys.* **2002**, *100*, 1261. (d) T. Kühn, H. Schwalbe, *J. Am. Chem. Soc.* **2000**, *122*, 6169.
11. C. Godard, P. L. Callaghan, J. L. Cunningham, S. B. Duckett, J. A. B. Lohman, R. N. Perutz, *Chem. Commun.* **2002**, 2836.
12. J. P. Dunne, D. Blazina, S. Aiken, H. A. Carteret, S. B. Duckett, J. A. Jones, R. Poli, A. C. Whitwood, *Dalton Trans.* **2004**, 3616.
13. (a) C. R. Bowers, D. P. Weitekamp, *J. Am. Chem. Soc.* **1987**, *109*, 5541. (b) T. C. Eisenschmid, R. U. Kirss, P. A. Deutsch, S. I. Hommeltoft, R. Eisenberg, J. Bargon, R. G. Lawler, A. L. Balch, *J. Am. Chem. Soc.* **1987**, *109*, 8089.
14. (a) J. Natterer, J. Bargon, *Prog. Nucl. Magn. Reson. Spectros.* **1997**, *31*, 293. (b) S. B. Duckett, C. J. Sleigh, *Prog. Nucl. Magn. Reson. Spectros.* **1999**, *34*, 71. (c) S. B. Duckett, D. Blazina, *Eur. J. Inorg. Chem.* **2003**, 2901. (d) D. Blazina, S. B. Duckett, J. P. Dunne, C. Godard, *Dalton Trans.* **2004**, 2601.
15. (a) A. Koch, J. Bargon, *Magn. Reson. Chem.* **2000**, *38*, 216. (b) M. Stephan, O. Kohlman, H. G. Niessen, A. Eichhorn, J. Bargon, *Magn. Reson. Chem.* **2002**, *40*, 157.
16. (a) S. A. Colebrooke, S. B. Duckett, J. A. B. Lohman, *Chem. Commun.* **2000**, 685. (b) S. A. Colebrooke, S. B. Duckett, J. A B. Lohman, *Chem. Eur. J.* **2004**, *10*, 2459.
17. (a) D. Blazina, S. B. Duckett, P. J. Dyson, J. A. B. Lohman, *Angew. Chem. Int. Ed.* **2001**, *40*, 3874. (b) R. Gobetto, L. Milone, F. Reineri, L. Salassa, A. Viale, E. Rosenberg, *Organometallics* 2002, **21**, 1919. (c) D. Blazina, S. B. Duckett, P. J. Dyson, J. A. B. Lohman, *Chem. Eur. J.* **2003**, *9*, 1046. (d) D. Blazina, S. B. Duckett, P. J. Dyson, J. A. B. Lohman, *Dalton Trans.* **2004**, 2108.
18. A. B. Permin, R. Eisenberg, *J. Am. Chem. Soc.* **2002**, *124*, 12406.
19. S. Aime, R. Gobetto, F. Raineri, D. Canet, *J. Chem. Phys.* **2003**, *119*, 8890.
20. J. Matthes, T. Perry, S. Grundemann, G. Buntkowsky, S. Sabo-Etienne, B. Chaudret, H. H. Limbach, *J. Am. Chem. Soc.* **2004**, *126*, 8366.
21. (a) M. S. Anwar, D. Blazina, H. A. Carteret, S. B. Duckett, T. K. Halstead, J. A. Jones, C. M. Kozak, R. J. K. Taylor, *Phys. Rev. Lett.* **2004**, *93*, 040501. (b) D. Blazina, S. B. Duckett, T. K. Halstead, C. M. Kozak, R. J. K. Taylor, M. S. Anwar, J. A. Jones, H. A. Carteret, *Magn. Reson. Chem.*, **2005**, *43*, 200.
22. C. H. Bennet, D. DiVincenzo, *Nature* **2000**, *404*, 247.
23. (a) M. S. Anwar, J. A. Jones, D. Blazina, S. B. Duckett, H. A. Carteret, *Phys. Rev. A* **2004**,*70*, 032324. (b) M. S. Anwar, D. Blazina, H. A. Carteret, S. B. Duckett, J. A. Jones, *J. Chem. Phys.*, **2004**, *400*, 94.
24. C. G. Kreiter, M. Lang, *J. Organomet. Chem.*, **1973**, *55*, C27
25. A. R. Rossi, R. Hoffman, Inorg. Chem. 1975, 14, 365.
26. T. Gottschalk-Gaudig, J. C. Huffman, K. G. Caulton. *J. Am. Chem. Soc.* **1999**, *121*, 3242.
27. M. Ogasawara, S. A. MacGregor, W. E. Streib, K. Polting, O. Eisenstein, K. G. Caulton, *J. Am. Chem. Soc.* **1995**, *117*, 8869.
28. D. Schott, J. P. Dunne, S. B. Duckett, C. Godard, J. N. Harvey, R. J. Mawby, G. Muller, R. N. Perutz, R. Poli, M. K. Whittlesey, *Dalton Trans.* **2004**, 3218.
29. J. P. Colman, W. R. Roper, *J. Am. Chem. Soc.* **1965**, *87*, 4008.
30. A. Anillo, R. Obeso-Rosete, M. A. Pellinghelli, A. Tiripicchio, *J. Chem. Soc., Dalton Trans.* **1991**, 2019.
31. (a) B. A. Messerle, C. J. Sleigh, M. G. Partridge, S. B. Duckett, *J. Chem. Soc., Dalton Trans.* **1999**, 1429. (b) P. Hubler, J. Bargon, *Angew. Chem. Int. Ed.* **2000**, *39*, 3701.
32. G. Bodenhausen, R. R. Ernst, *J. Am. Chem. Soc.* **1982**, *104*, 1304.

33. D. Blazina, S. B. Duckett, P. J. Dyson, B. F. G. Johnson, J. A. B. Lohman, C. J. Sleigh, *J. Am. Chem. Soc.* **2001**, *123*, 9760.
34. Gaussian 03, Revision B.05. M. J. Frisch, G. W. Trucks, H. B. Schlegel, G. E. Scuseria, M. A. Robb, J. R. Cheeseman, J. A. Montgomery, Jr., T. Vreven, K. N. Kudin, J. C. Burant, J. M. Millam, S. S. Iyengar, J. Tomasi, V. Barone, B. Mennucci, M. Cossi, G. Scalmani, N. Rega, G. A. Petersson, H. Nakatsuji, M. Hada, M. Ehara, K. Toyota, R. Fukuda, J. Hasegawa, M. Ishida, T. Nakajima, Y. Honda, O. Kitao, H. Nakai, M. Klene, X. Li, J. E. Knox, H. P. Hratchian, J. B. Cross, C. Adamo, J. Jaramillo, R. Gomperts, R. E. Stratmann, O. Yazyev, A. J. Austin, R. Cammi, C. Pomelli, J. W. Ochterski, P. Y. Ayala, K. Morokuma, G. A. Voth, P. Salvador, J. J. Dannenberg, V. G. Zakrzewski, S. Dapprich, A. D. Daniels, M. C. Strain, O. Farkas, D. K. Malick, A. D. Rabuck, K. Raghavachari, J. B. Foresman, J. V. Ortiz, Q. Cui, A. G. Baboul, S. Clifford, J. Cioslowski, B. B. Stefanov, G. Liu, A. Liashenko, P. Piskorz, I. Komaromi, R. L. Martin, D. J. Fox, T. Keith, M. A. Al-Laham, C. Y. Peng, A. Nanayakkara, M. Challacombe, P. M. W. Gill, B. Johnson, W. Chen, M. W. Wong, C. Gonzalez,, J. A. Pople, Gaussian, Inc., Pittsburgh PA, 2003.
35. J. Harvey, M. Aschi, *Faraday Disc.*, **2003**, *124*, 129
36. A. D. Becke, *J. Chem. Phys.* **1993**, *98*, 5648–5652.
37. A. Schaefer, H. Horn, R. Ahlrichs, *J. Chem. Phys.* **1992**, *97*, 2571–2577.
38. J. N. Harvey, R. Poli, *Dalton Trans.*, **2003**, *21*, 4100
39. J. N. Harvey, M. Aschi, *Faraday Disc.*, **2003**, *124*, 129
40 M Ogasawara, F. Maseras, N. Gallego-Plana, W. E. Streib, O. Eisenstein, K. G. Caulton. *Inorg. Chem.* **1996**, *35*, 7468.
41. M Ogasawara, F. Maseras, N. Gallego-Plana, K. Kawamura, K. Ito, K. Toyota, W. E. Streib, S. Komiya, O. Eisenstein, K. G. Caulton. *Organometallics.* **1997**, *16*, 1979.
42. D. Schott. C. J. Sleigh, J. P. Lowe, S. B. Duckett, R. J. Mawby, *Inorg. Chem.* 2002, **41**, 2960.
43. Following IUPAC nomenclature.
44. (a) C. W. Jung, P. E. Garrou, *Organometallics* **1982**, *4*, 659. (b) H. Kawano, R. Tanaka, T. Fujikawa, K. Hiraki, M. Onishi. *Chem. Lett.*, **1999**, 401.
45. (a) B. T. Heaton, J. A. Iggo, I. S. Podkorytov, D. J. Smawfield, S. P. Tunik, R. Whyman, *J. Chem. Soc., Dalton Trans.* **1999**, 1917; (b) D. S. Z. Sabounchei, B. T. Heaton, J. A. Iggo, C. Jacob, I. S. Podkorytov, *J. Clust. Sci.* **2001**, *12*, 339.
46. T. G. Prestwich, D. Blazina, S. B. Duckett, P. J. Dyson, *Eur. J. Inorg. Chem.* **2004**, 4381.
47. V. Montiel-Palma, D. I. Pattison, R. N. Perutz, C. Turner, *Organometallics* **2004**, *23*, 4034.
48. S. A. Macgregor, O. Eisenstein, M. K. Whittlesey, R. N. Perutz, Dalton. **1988**, 291.
49. A. L. Sargent, M. B. Hall, *Inorg. Chem.*, **1992**, *31*, 317.
50. P. Meakin, E. L. Muetterties, J. P. Jesson, *J. Am. Chem. Soc.*, **1973**, *95*, 75.
51. P. Meakin, E. L. Muetterties, F. N. Tebbe, J. P. Jesson, *J. Am. Chem. Soc.*, **1971**, *93*, 4701.
52. J. P. Jesson, E. L. Muetterties, P. Meakin, *J. Am. Chem. Soc.*, **1971**, 93, 5261.
53. G. E. Ball, B. E. Mann, *J. Chem. Soc., Chem. Commun.*, **1992**, 561.
54. R. G. Pearson, H. W. Walker, H. Mauermann, P. C. Ford, *Inorg. Chem.*, **1981**, *20*, 2743.
55. D. F. Brougham, D. A. Brown, N. J. Fitzpatrick, W. K. Glass, *Organometallics*, **1995**, *14*, 151.
56. A. Dedieu, S. Nakamura, *J. Organomet. Chem.*, **1984**, *260*, C63.
57. V. Bakhmutov, T. Burgi, P. Burger, U. Ruppli, H. Berke, *Organometallics*, **1994**, *13*, 4203.